Quantitative Analysis of the Ellipsoid Zone Intensity in Phenotypic Variations of Intermediate Age-Related Macular Degeneration

Thomas J. Gin,[1] Zhichao Wu,[1] Sky K. H. Chew,[1] Robyn H. Guymer,[1,2] and Chi D. Luu[1,2]

[1]Centre for Eye Research Australia, Royal Victorian Eye and Ear Hospital, Melbourne, Victoria, Australia
[2]Department of Surgery (Ophthalmology), The University of Melbourne, Melbourne, Victoria, Australia

Correspondence: Chi D. Luu, Centre for Eye Research Australia, Level 8, 32 Gisborne Street, East Melbourne, Victoria 3002, Australia; cluu@unimelb.edu.au.

RHG and CDL are joint senior authors.

Submitted: June 9, 2016
Accepted: March 9, 2017

Citation: Gin TJ, Wu Z, Chew SKH, Guymer RH, Luu CD. Quantitative analysis of the ellipsoid zone intensity in phenotypic variations of intermediate age-related macular degeneration. *Invest Ophthalmol Vis Sci.* 2017;58:2079–2086. DOI:10.1167/iovs.16-20105

Purpose. Reduction of the ellipsoid zone (EZ) intensity has been reported in eyes with age-related macular degeneration (AMD). This study determined whether overall EZ intensity, in retinal locations undisturbed by pathologic features, is associated with the presence of clinical features, which are known important phenotypic risk factors for disease progression, large drusen, reticular pseudodrusen (RPD), and pigmentary abnormalities.

Methods. A horizontal B-scan through the foveola on spectral-domain optical coherence tomography (SD-OCT) was performed in both eyes of 75 participants with bilateral intermediate AMD and 10 age-similar control participants. Eyes with AMD were classified as per the presence of large drusen, RPD, and hyperpigmentary changes. The relative EZ intensity profile, up to an eccentricity of 3400 μm, was averaged over seven 1000-μm retinal segments. The association between relative EZ intensity profile over seven retinal segments and AMD pathologic features was analyzed.

Results. The average relative EZ intensities were significantly reduced in eyes with intermediate AMD compared to normal eyes ($P \leq 0.025$) and with increasing age ($P \leq 0.020$). On multivariate analyses, only the presence of hyperpigmentary changes and increasing age were significantly associated with reduced overall relative intensities ($P \leq 0.024$), but not the presence of large drusen or RPD ($P \geq 0.115$).

Conclusions. The presence of hyperpigmentary change in the macula in association with large drusen, not large drusen alone, nor large drusen with RPD, was significantly associated with a generalised reduction in EZ intensity. Quantitative assessment of the relative EZ intensity may serve as an effective biomarker of disease severity and progression.

Keywords: age-related macular degeneration, spectral-domain optical coherence tomography, ellipsoid zone, inner-segment ellipsoids, reticular pseudodrusen

Clinical classification systems of the early stages of age-related macular degeneration (AMD), based on drusen and pigmentary changes on color fundus photography, are conventionally used to stratify risk of progression toward developing vision threatening, advanced changes including neovascularization and geographic atrophy (GA).[1–3] In recent years, reticular pseudodrusen (RPD; also referred to as subretinal drusenoid deposits) have also been suggested as an additional risk for the development of late stage disease.[4,5]

Further characterization of early pathologic changes revealed on high-resolution spectral-domain optical coherence tomography (SD-OCT) offers us an opportunity to identify other structural biomarkers of disease severity. We and others have suggested a role for the second hyperreflective band, seen in the outer retina, as a marker of disease severity in various inflammatory diseases[6–8] as well as retinal inherited and degenerative conditions.[9–11] Although previously referred to as the inner segment-outer segment (IS/OS) junction, the reflectivity of this band has more recently been suggested to originate from the photoreceptor IS ellipsoids,[12,13] thus it was referred to as the ellipsoid zone (EZ) at a recent international OCT nomenclature meeting.[14] The photoreceptor IS ellipsoids are densely packed with mitochondria, and have important metabolic and light guiding roles. In eyes with AMD, disruption to the integrity of this band has been significantly associated with reduced visual acuity[15,16] and microperimetric retinal sensitivity.[17–19] The integrity of the EZ has been suggested as a prognostic indicator for vision in central serous chorioretinopathy,[20] retinal vein occlusion,[21] and following intravitreal antivascular endothelium growth factor therapy for neovascular AMD.[22–24]

However, assessment of the EZ has largely been limited to qualitative grading of its integrity, which involves noting its presence, absence, or the degree of disruption.[25] More recently, Hood et al.[11] expanded this by quantitatively measuring the intensity of the EZ, showing a reduction in intensity (despite a relatively normal-appearing band) in patients with diminished cone function. We also subsequently found that the intensity of the EZ was reduced in eyes with the early stages of AMD compared to normal, aged-matched eyes,[26] and its intensity was associated with functional changes determined using multifocal electroretinography.[27] However, the differences in the EZ intensity in the presence of different pathologic features in intermediate AMD remain to be

determined, and could provide insights into its potential utility as a clinical biomarker.

We therefore sought to examine whether the intensity of the EZ, in retinal locations undisturbed by pathologic features, was associated with features, typical in intermediate AMD, which are known important phenotypic risk factors for disease progression, including the presence of large drusen, hyperpigmentation, and RPD. Alteration in the intensity of the EZ may provide a new quantifiable clinical biomarker of disease severity and risk of progression to vision loss in eyes with intermediate AMD.

Methods

This study was approved by the Human Research Ethics Committee of the Royal Victorian Eye and Ear Hospital (RVEEH) and was conducted in adherence with the Declaration of Helsinki. All participants provided written informed consent after an explanation of all test procedures.

Participants

Participants with AMD were recruited from AMD research clinics at the Centre for Eye Research Australia. Spouses and friends of the AMD participants were recruited as control participants for this study. Inclusion criteria for all participants were to be over 50 years of age and to have best-corrected visual acuity of better than 20/40 (0.30 logarithm of the minimum angle of resolution [logMAR]). The inclusion criteria for AMD participants included having drusen >125 μm, with or without pigmentary abnormalities in both eyes (intermediate AMD).[28] Control participants were included only if both eyes did not exhibit signs of AMD, although drusen ≤63 μm were allowed (normal aging changes).[28] The exclusion criteria for any participants included the presence of any GA, choroidal neovascularization (CNV), significant cataracts, glaucoma, amblyopia, and any corneal pathology that could compromise vision in either eye. Participants were also excluded if they had diabetes or any neurologic or systemic disease affecting vision, were taking any medication known to affect retinal or visual function (e.g., hydroxychloroquine), if they had any physical and/or mental impairment preventing them from participating, or were unable to, or did not provide written informed consent. Both eyes of each participant were included in this study.

Imaging

Colour fundus photographs were obtained with a Canon nonmydriatic camera (Canon CR6-45NM; Canon, Saitama, Japan). Near-infrared reflectance, fundus autofluorescence imaging, and SD-OCT high-resolution line and volume scans were obtained using a Spectralis HRA+OCT (Heidelberg Engineering, Heidelberg, Germany). The SD-OCT volume scan was performed using 49 B-scans that covered a 20° × 20° area using the high-resolution setting and averaging 25 frames for each B-scan to grade the presence of RPD and assist the detection of any SD-OCT defined GA.[29,30] The SD-OCT horizontal line scan through the fovea was performed using the high-resolution setting and image averaging of 100 frames. All SD-OCT scans were performed with the zero delay set at the vitreous level (being the default setting).

Analysis of Pathologic Features

In this study, pathologic features were analyzed and graded within the central 6000 μm diameter, centred on the fovea, to allow consistency to be achieved across imaging modalities. All images were graded by one senior grader (Khin Zaw Aung) who was masked to the EZ intensity results. Color fundus photographs were graded in accordance with a recently revised Beckman AMD classification.[28] Using color fundus photographs, the presence of intermediate AMD was defined as drusen >125 μm in the area 6000 μm in diameter centered on the fovea. Hyperpigmentary changes were defined when hyperpigmented clumps were visible on color fundus photography within the area 6000 μm in diameter centered on the fovea.[28] Hypopigmentary changes were not accounted for in this study. The presence of RPD was defined as groups of hyporeflective lesions against a background of mild hyperreflectance on near-infrared reflectance (NIR), with corresponding hyperreflective signal above the retinal pigment epithelium on SD-OCT volume scans.[31–33] The co-localization of RPD on these two imaging modalities was evaluated qualitatively on the software of the device, noting the potential for co-localization errors as reported previously.[34] Only those graded as having definite RPD were considered as having RPD.

Analysis of the EZ

The logarithmic-transformed display of the B-scan (horizontal SD-OCT line scan through the fovea), for each eye of each participant, was exported in tagged image file format (TIFF) using the Heidelberg Eye Explorer software (version 1.9.10.0, Heidelberg Engineering). The transformed image was chosen for analysis to enable accurate manual sampling of the retinal microstructure. This should be distinguished from linear (raw) reflectivities, which other authors have used to evaluate automated algorithms. These raw images are more difficult for human evaluators to interpret and manually sample.[35] The optical coherence tomography images in TIFF were then uploaded into Igor Pro (WaveMetrics, Lake Oswego, OR, USA) computer software for analyzing the relative intensity of the EZ band. The ellipsoid zone grading and analysis was performed by a single experienced examiner (TJG) who was not involved in grading the images for AMD phenotype, and thus was masked to the AMD phenotype grading results during the grading and analysis of the EZ. As defined by the recently proposed nomenclature meeting,[14] the EZ (previously referred to as the IS ellipsoid band or IS/OS junction), external limiting membrane (ELM), and inner nuclear layer (INL) were each manually sampled at each retinal location of interest. A total of 35 retinal locations were sampled; at the fovea and at 200-μm intervals, to a maximum eccentricity of 3400 μm from the fovea, both nasally and temporally, and the gray value of the pixel sampled (ranging from 0 to 255) for each OCT band of interest was recorded.

The relative intensity of the EZ was determined as a ratio of the intensity of the EZ to the ELM and INL at each retinal location. To ensure differences in the relative intensity can be ascribed to differences in the EZ, two references were selected. The external limiting membrane and INL were selected for reference because these layers are considered to be the least altered in early disease and their intensities are relatively constant across a wide eccentricity.[27,36] Other authors have suggested the use of the vitreous or retinal nerve fiber layer (RNFL) as a reference for intensity profiles.[37,38] We avoided using the vitreous as a reference given the reflectivity of this region depended on the presence of a posterior vitreous detachment. We also avoided the use of the RNFL given the potential for early glaucomatous changes to potentially impact on the RNFL reflectivity,[39] that may be undetected on the clinical examination of the optic nerve.

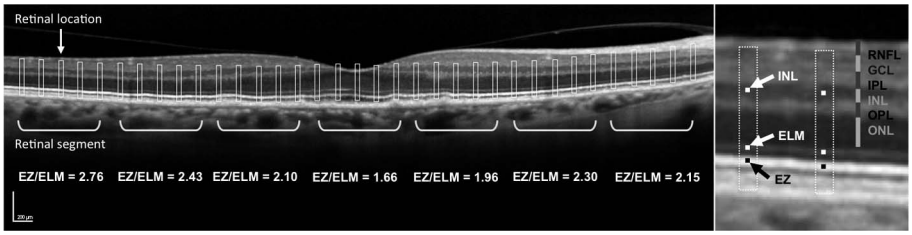

Figure 1. Diagram illustrating the 35 retinal locations where the EZ, ELM, and INL were sampled; at the fovea and at 200 μm intervals, to a maximum eccentricity of 3400 μm from the fovea, both nasally and temporally. The relative intensity of the EZ was determined as a ratio of the EZ to the ELM and INL. The relative EZ intensity was then averaged over each of the seven 1000-μm horizontal retinal segments, each consisting of five retinal locations. This diagram illustrates the seven 1000-μm horizontal retinal segments and their corresponding average EZ/ELM ratios.

To avoid the local "shadowing" effect of retinal vessels on the underlying EZ, ELM, INL, retinal locations affected by local vessel "shadowing" were not chosen for analysis. To avoid the possible local effect of drusen, RPD and hyperreflective foci on the reflective properties of EZ, ELM, or INL (as a result of local disruption[25] or alterations in the angle of incidence of light[40]), only retinal locations, along the horizontal foveal scan, that exhibited no disturbance associated with these pathologic features, within 50 μm, were chosen for analysis. Hyperreflective foci were defined on SD-OCT as lesions of equal or higher reflectivity than the RPE band, located within the neurosensory retina, often discrete and well-circumscribed, but sometimes seen attached to elevated RPE overlying drusen.[41] The relative EZ intensity at each retinal location was then averaged over each of the seven 1000-μm horizontal retinal segments, each consisting of five retinal locations, as shown in Figure 1. Eyes that exhibited disruption across all five retinal locations, in three or more retinal segments, were excluded to ensure statistical validity. Of note, as the INL was absent at the fovea, the EZ/INL ratio could not be calculated at the fovea. Thus, the mean EZ/INL ratio of the central retinal segment (zero eccentricity) was averaged only from 4/5 retinal locations sampled at 200 and 400 μm on either side of the fovea where the INL was discernible.

Statistical Analysis

An independent samples *t*-test was used to examine the difference in age between the participants with intermediate AMD and normal participants. Linear mixed-effects models (LMMs) were then used to compare the outcome parameters (EZ/ELM, EZ/INL, and ELM/INL) between eyes with and without the clinical features of intermediate AMD. These models are used to account for the hierarchical nature of the data, and are therefore ideal for this data.[42] The general form of the model for each measurement of the intensity ratio (a) at each location (b) nested within an eye (c), nested within a patient (d) was as follows:

$$\text{Intensity Ratio}_{abcd} = \beta_0 + \beta_1 \times \text{Age} + \beta_2 \times \text{Diagnosis} + \zeta_{b/c} + \zeta_{b/c/d} + \varepsilon_{abcd}$$

Where β_0 through to β_2 represents the fixed effects associated with the intercept, age, and diagnosis of AMD, $\zeta_{b/c}$ and $\zeta_{b/c/d}$ represents the random eye nested within patient and location nested within eye nested within patient effects, respectively, and ε_{abcd} represents the residual. A similar model was subsequently built to allow multivariate analyses to be performed, which allowed the presence of each AMD pathologic feature (large drusen, RPD, and hyperpigmentation) to be included separately.

Results

A total of 75 participants with bilateral intermediate AMD were recruited for this study, of which 10 patients had eyes that exhibited disruption across all five retinal locations in three or more retinal segments and were not included in the analysis. A total of 65 participants with bilateral intermediate AMD (71.3 ± 6.8 years, range 51–85) and 10 controls (69.9 ± 9.1 years, range 53–86) were included in the final analysis. There was no significant difference in age between control participants and those with the clinical features of intermediate AMD ($P = 0.646$). The number of eyes with different AMD phenotypes, based on the presence of large drusen, RPD, and hyperpigmentation, is shown in Table 1.

Representative OCT scans in Figure 2 illustrate qualitatively and quantitatively the difference in EZ/ELM ratios in a control eye and the different phenotypic variations of intermediate AMD. Both EZ/ELM and EZ/INL ratios exhibited regional variation with characteristic minima at the foveal region (Fig. 3).[11,27] Examining all participants, the EZ/ELM and EZ/INL ratios were significantly reduced in eyes with intermediate AMD compared to normal eyes ($P \leq 0.025$) and also reduced with increasing age ($P \leq 0.020$). However, the ELM/INL ratio was not significantly different between eyes with intermediate AMD compared to normal eyes ($P = 0.855$) and did not change significantly with age ($P = 0.444$; Table 2).

To further examine which pathologic features were associated with an overall reduction in relative intensity of the EZ, multivariate analyses were performed. Only the additional presence of hyperpigmentation and increasing age were significantly associated with reduced overall EZ/ELM and EZ/INL ($P \leq 0.024$), but not the presence of large drusen alone or the additional feature of RPD ($P \geq 0.115$). There were no factors significantly associated with a reduced ELM/INL ratio ($P \geq 0.382$; Table 3). The mean EZ/ELM ratios for our intermediate AMD eyes, categorized by AMD phenotype, with comparison made to normal eyes, are shown in Figure 4.

Discussion

We have previously suggested that the intensity of the EZ may provide a marker of disease severity in nonneovascular

Table 1. Number of Eyes With Different AMD Phenotypes Included in This Study

AMD Phenotypes	Number of Eyes (%)
Large drusen only	64 (49)
Large drusen and RPD	32 (25)
Large drusen and hyperpigmentation	25 (19)
Large drusen, RPD, and hyperpigmentation	9 (7)

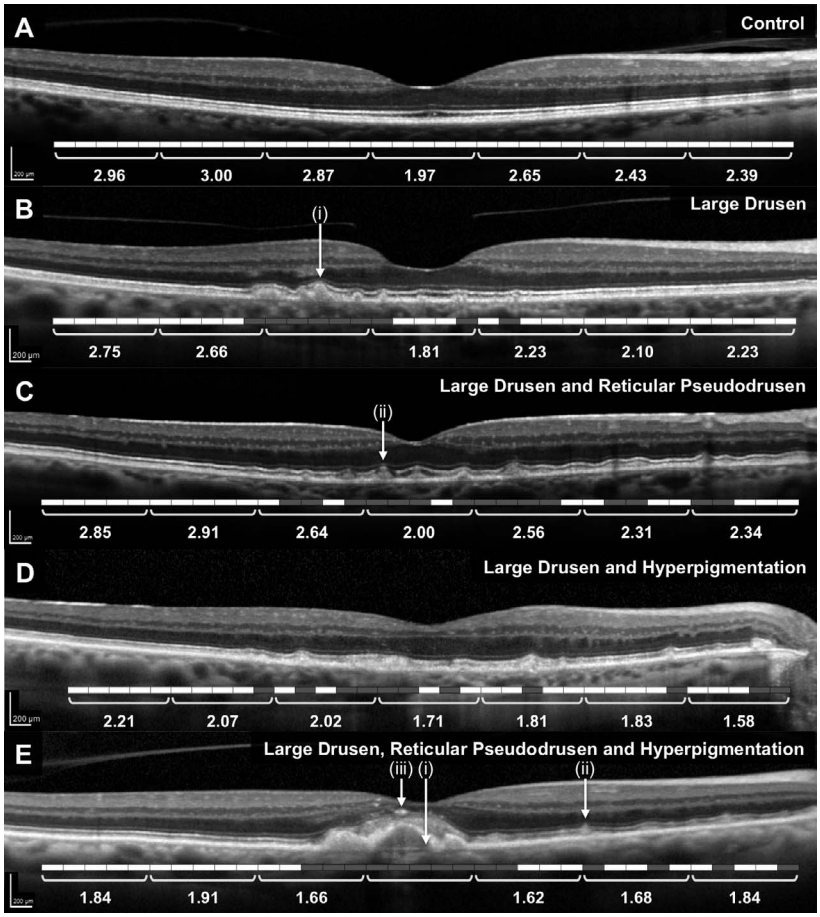

Figure 2. Representative high-resolution horizontal line OCT scans through the fovea and mean relative intensities of the EZ relative to the ELM in a control eye (**A**) and eyes graded to have different intermediate AMD phenotypes; large drusen only (>125 μm; **B**), large drusen and RPD (**C**), large drusen and hyperpigmentation (**D**), and large drusen, RPD and hyperpigmentation (**E**). Examples of drusen (i), RPD (ii), and hyperreflective foci (iii) are indicated by the *arrows*. Beneath each OCT scan, are *bars* corresponding to the 35 retinal locations sampled at 200-μm intervals. Only retinal locations that exhibited no disruption associated with pathologic features were chosen for analysis and are labeled with a corresponding *white bar*. Retinal locations exhibiting disruption, not included in the analysis, are labeled with a *black bar*. The mean EZ/ELM ratio for each retinal segment is shown below the corresponding retinal segment. Note that one retinal segment from both **B** and **E** OCT scans is absent, as all five retinal locations in these retinal segments exhibited disruption secondary to pathology and were not included in the analysis.

AMD.[26,27] We found the average relative EZ intensity was lower in a cohort of eyes with AMD, displaying a broader range of nonneovascular AMD phenotype than this current report, when compared to normal, similar-aged eyes. We also reported that reduced intensity of the EZ was significantly associated with a delay in the multifocal electroretinogram (mfERG) implicit time.[27] However, further evaluation of how the EZ intensity differs in the presence of different pathologic features in intermediate AMD could provide further insights into its potential utility as a clinical biomarker. Thus, we sought to examine the association between overall EZ intensity, in retinal locations undisturbed by pathologic features, and the presence of different clinical features present within the macula of a uniform group of participants with intermediate AMD.

It is important to note that our study did not examine the association between AMD phenotypes and localized EZ

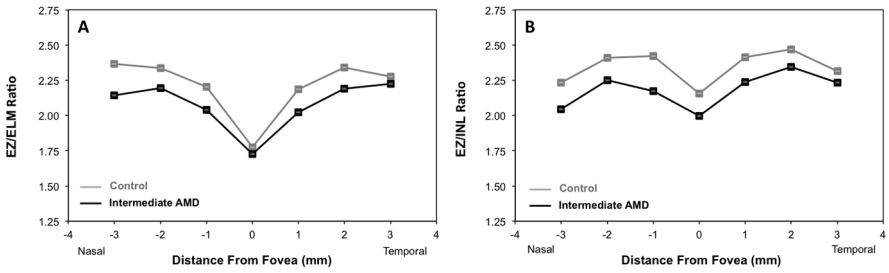

Figure 3. Comparison of the relative intensity of the EZ, averaged over the seven retinal segments, between intermediate AMD subjects (*black*) and controls (*gray*) with the EZ as a ratio of the ELM (**A**) and INL (**B**). The relative EZ intensity was reduced in eyes with intermediate AMD compared to normal eyes ($P \leq 0.025$), and both EZ/ELM and EZ/INL ratios exhibited regional variation with characteristic minima at the foveal region.

Table 2. Relative Intensity of the EZ on SD-OCT Compared Between Eyes With and Without the Features of Intermediate AMD

Parameters	Estimate	95% Confidence Interval	*P* Value
EZ/ELM ratio			
Intercept	2.53	2.07 to 3.00	<0.001
Age (per decade)	−0.06	−0.12 to −0.01	0.020
Diagnosis (AMD)	−0.13	−0.24 to −0.02	0.025
EZ/INL ratio			
Intercept	2.74	2.27 to 3.22	<0.001
Age (per decade)	−0.08	−0.14 to −0.02	0.013
Diagnosis (AMD)	−0.15	−0.28 to −0.02	0.020
ELM/INL ratio			
Intercept	1.11	0.95 to 1.27	<0.001
Age (per decade)	0.00	−0.02 to 0.01	0.444
Diagnosis (AMD)	0.00	−0.04 to 0.04	0.855

Table 3. Impact of the Presence of Different Pathological Features in Intermediate AMD on the Relative Intensity of the EZ on SD-OCT

Parameters	Estimate	95% Confidence Interval	*P* Value
EZ/ELM ratio			
Intercept	2.39	1.91 to 2.87	<0.001
Age (per decade)	−0.06	−0.12 to −0.01	0.024
Large drusen*	−0.08	−0.19 to 0.04	0.181
RPD*	−0.07	−0.18 to 0.02	0.115
Hyperpigmentation*	−0.11	−0.20 to −0.02	0.022
EZ/INL ratio			
Intercept	2.63	2.13 to 3.13	<0.001
Age (per decade)	−0.08	−0.14 to −0.02	0.012
Large drusen*	−0.11	−0.24 to 0.03	0.122
RPD*	−0.05	−0.15 to 0.06	0.372
Hyperpigmentation*	−0.13	−0.23 to −0.02	0.020
ELM/INL ratio			
Intercept	1.13	0.96 to 1.30	<0.001
Age (per decade)	−0.01	−0.03 to 0.01	0.382
Large drusen*	−0.01	−0.05 to 0.03	0.725
RPD*	0.01	−0.02 to 0.04	0.439
Hyperpigmentation*	0.00	−0.03 to 0.03	0.990

* Presence of the feature analyzed.

changes related to specific pathologic features. Whilst previous studies have qualitatively graded the focal elevation, disruption, and absence of the EZ directly overlying drusen,[25,43,44] and RPD,[31,32,45,46] our study set out to quantify EZ through a consistent, horizontal section in a scan through the fovea in all participants and its association with the clinical phenotype represented by the presence of each AMD pathologic feature. To avoid the possible effect of drusen, RPD, and hyperreflective foci on the local reflective properties of EZ, ELM, or INL, we specifically sought to only examine retinal locations where the EZ was not disturbed due to pathologic features. Including these retinal locations, overlying lesions could capture EZ reflectivity changes as a result of local EZ disruption,[25] or alterations in the angle of incidence of light as a result of lesion-associated elevation,[40] rather than providing an exclusive evaluation of overall EZ intensity that is comparable across the different eyes examined in this study.

We found that the average relative EZ intensity, as measured on the horizontal line scan passing through the fovea, is lower in eyes with intermediate AMD compared to normal aged eyes, which is consistent with our previous findings within 1000 μm of the fovea in nonneovascular AMD eyes with a wider range of disease severity.[27] The current study further revealed that it was only when the clinical phenotype includes macular hyperpigmentation in association with large drusen, not large drusen alone (>125 μm) or large drusen and RPD, that was significantly associated with a generalized reduction in EZ intensity. Our findings suggest that the presence of hyperpigmentation in the macula in AMD, a sign of distressed, dying, or dead RPE cells,[47] is a significant change in the severity of the disease profile, correlating with what we assume to be an indicator of outer retinal health—a less intense EZ.

Numerous epidemiologic studies have demonstrated AMD eyes with drusen >125 μm, with macular pigmentary changes, are at a greater risk of vision loss than similarly graded AMD eyes without these features.[1–3] Recent SD-OCT findings further support that hyperpigmentary changes (seen as hyperreflective foci[48]) are pathologic markers of disease severity that proliferate significantly and migrate over time—characteristics that are associated with a greater incidence of GA.[47] The significant association between reduced overall EZ intensity and the presence of hyperpigmentation with large drusen agrees with these reports.

The absence of a significant association between EZ intensity through the foveal scan and the presence of large drusen only, or large drusen and RPD, suggests that the outer retinal health is not as affected in these clinical phenotypes. The actual pathologic processes involved in the formation of RPD, and their effect on the AMD process, is still not well understood but is the subject of much investigation.[31,32] At least from our observations presented here, they do not appear to affect the intensity of the EZ as measured through the central scan, to the same extent as the presence of hyperpigmentation. It is also possible that changes in EZ intensity may be more apparent as the RPD occupy a greater area,[45,46] or when they are present in the foveal scan being analyzed, or if the SD-OCT scans being analyzed are specifically through the locations that harbor the RPD lesions.

In interpreting our findings of an absence of a significant association between overall EZ intensity and the presence of large drusen only, or large drusen and RPD, it is important to note that our intermediate AMD eyes with pathologic changes that disrupted the EZ across all retinal locations of at least three retinal segments were not included in the analysis. Intermediate AMD eyes with confluent drusen across >3000 μm of the horizontal foveal OCT scan were not represented in this study.

EZ reflectivity may, in part, reflect mitochondrial integrity within the photoreceptor IS ellipsoid. Emerging evidence has suggested a key role for mitochondrial dysfunction in the AMD pathogenesis with the mitochondrial genome shown to impact AMD susceptibility.[49,50] As mitochondria comprise up to 74% to 85% of cone ellipsoids,[51] whether the IS ellipsoids coincide with the SD-OCT EZ remains of key interest and debate.[52,53] Reflectivity of photoreceptors on SD-OCT has been postulated to originate from light scattering or waveguiding.[54,55] Mitochondria have been identified as an organelle potentially responsible for photoreceptor reflectivity, as they powerfully scatter light in vitro.[13] In addition, recent clinical pathologic correlations between SD-OCT findings and mitochondrial translocation in degenerating cones, in the late stages of AMD, support the notion that these SD-OCT photoreceptor reflectivity changes could be attributed to changes in photoreceptor mitochondrial distribution.[55–57] If mitochondria do contribute to EZ reflectivity, EZ intensity may serve as a surrogate marker of IS mitochondrial integrity. A quantitative marker of IS mitochondrial wellbeing, and thus photoreceptor

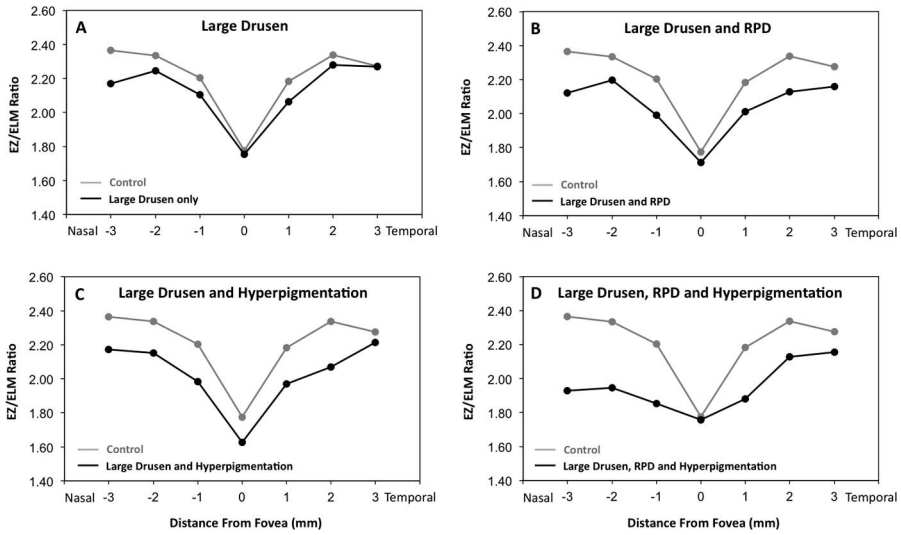

Figure 4. Comparison of the mean intensity of the EZ relative to the ELM between control eyes (*gray*) and eyes with the different intermediate AMD phenotypes (*black*); large drusen (>125 μm; **A**), large drusen and RPD (**B**), large drusen and hyperpigmentation (**C**), and large drusen, RPD, and hyperpigmentation (**D**). On multivariate analyses, only the presence of hyperpigmentary changes and increasing age were significantly associated with reduced overall relative intensities, but not the presence of large drusen or RPD. Points nasal and temporal to the fovea are represented by negative and positive values, respectively.

health, may prove significant in determining those at risk of progression to vision loss in the earlier stages of AMD.

Although manual selection of a single pixel for the determination of the intensity at each retinal location of interest (EZ, ELM, or INL), in contrast to the measurement of the peak intensity over five pixels horizontally performed previously,[26,27] may increase variability in the measurement of intensity, the consistency of our findings with previous reports, we believe, validates our novel method of quantifying band intensity. Prudent selection of the single pixel at each location of interest allowed for rapid characterization of intensity over a broad retinal region. Consistent with previous reports, the relative EZ intensity varied with eccentricity reaching a minimum at the fovea.[11] This may be due to the increase in ellipsoid volume with increasing eccentricity[51] and the absence of rods at the fovea, which also contributes to the intensity of the EZ band.[11,58] To accommodate for the automatic brightness adjustments to SD-OCT images, the ELM and INL were chosen as references. These structures are considered to remain relatively unaltered in early disease.[27] In our study, similar findings were obtained irrespective of whether the ELM or the INL was used as the reference layer. We selected the ELM as our preferred reference to present our study results, as, unlike the INL, the ELM is present at the foveola, and could be sampled in all eyes. The external limiting membrane/inner nuclear layer ratio was neither significantly different between cohorts nor associated with age or the presence of any of the AMD pathologic features. These findings align with our previous results that show ELM and INL intensities appear unaltered in eyes with intermediate AMD,[27] and, together with the similar results between EZ/ELM and EZ/INL ratios, validate that the differences in relative intensity found, can be ascribed to the EZ. Although averaging EZ/ELM intensities across the central retinal segment may have included the nadir of EZ intensity corresponding to the fovea, as the INL is absent at the fovea, the average EZ/INL of the central retinal segment omitted the foveal EZ/INL intensity in all eyes. Given the agreement of both EZ/INL and EZ/ELM ratios, independent analysis of the foveal EZ/ELM is unlikely to have a significant effect for the purposes of evaluating overall EZ intensity in this study.

The current study performs an initial cross-sectional characterization of overall EZ intensity in the intermediate stage of disease using a single horizontal B-scan, and future automated analyses, using the EZ obtained from the entire volume scan in longitudinal data, and evaluation against quantitative measures of pathologic changes (such as drusen volume), will permit more robust conclusions about the utility of the EZ as a single biomarker of disease severity and progression. Software algorithms, which can provide automated measurements of peak band intensity (such as the method recently developed by Ross and colleagues[35]), may prove more accurate and allow rapid characterization of sequential scans.

Conclusions

Intermediate AMD phenotypes with macular hyperpigmentation in association with large drusen, not large drusen alone (>125 μm), nor large drusen and RPD, were significantly associated with a generalized reduction in EZ intensity. Longitudinal studies are required to determine whether alteration in this new quantifiable structural biomarker may serve to provide an effective marker of disease severity in clinical practice.

Acknowledgments

The authors thank Khin Zaw Aung for his assistance in image grading.

Supported by the National Health and Medical Research Council (NH&MRC) Project Grants (1084081, 1027624). Centre for Eye Research Australia (CERA) receives operational infrastructure support from the Victorian Government.

Disclosure: **T.J. Gin**, None; **Z. Wu**, None; **S.K.H. Chew**, None; **R.H. Guymer**, None; **C.D. Luu**, None

References

1. Klein R, Davis MD, Magli YL, Segal P, Klein BE, Hubbard L. The Wisconsin age-related maculopathy grading system. *Ophthalmology.* 1991;98:1128–1134.

2. Ferris FL, Davis MD, Clemons TE, et al. A simplified severity scale for age-related macular degeneration - AREDS report no. 18. *Arch Ophthalmol*. 2005;123:1570–1574.
3. Anand R, Bressler SB, Davis MD, et al. Risk factors associated with age-related macular degeneration - a case-control study in the Age-Related Eye Disease Study: Age-Related Eye Disease Study report number 3. *Ophthalmology*. 2000;107:2224–2232.
4. Finger RP, Wu Z, Luu CD, et al. Reticular pseudodrusen. *Ophthalmology*. 2014;121:1252–1256.
5. Arnold JJ, Sarks SH, Killingsworth MC, Sarks JP. Reticular pseudodrusen. A risk factor in age-related maculopathy. *Retina*. 1995;15:183–191.
6. Hashimoto H, Kishi S. Ultra-wide-field fundus autofluorescence in multiple evanescent white dot syndrome. *Am J Ophthalmol*. 2015;159:698–706.e691.
7. Lee GE, Lee BW, Rao NA, Fawzi AA. Spectral domain optical coherence tomography and autofluorescence in a case of acute posterior multifocal placoid pigment epitheliopathy mimicking Vogt-Koyanagi-Harada disease: case report and review of literature. *Ocul Immunol Inflamm*. 2011;19:42–47.
8. Chai Y, Yamazaki H, Fujinami K, Tsunoda K, Yamamoto S. Case of acute zonal occult outer retinopathy with abnormal pattern visual evoked potentials. *Clin Ophthalmol*. 2011;5:1235–1241.
9. Tao LW, Wu Z, Guymer RH, Luu CD. Ellipsoid zone on optical coherence tomography: a review. *Clin Experiment Ophthalmol*. 2015;44:422–430.
10. Cai CX, Locke KG, Ramachandran R, Birch DG, Hood DC. A comparison of progressive loss of the ellipsoid zone (EZ) band in autosomal dominant and x-linked retinitis pigmentosa. *Invest Ophthalmol Vis Sci*. 2014;55:7417–7422.
11. Hood DC, Zhang X, Ramachandran R, et al. The inner segment/outer segment border seen on optical coherence tomography is less intense in patients with diminished cone function. *Invest Ophthalmol Vis Sci*. 2011;52:9703–9709.
12. Fernandez EJ, Hermann B, Povazay B, et al. Ultrahigh resolution optical coherence tomography and pancorrection for cellular imaging of the living human retina. *Opt Express*. 2008;16:11083–11094.
13. Spaide RF, Curcio CA. Anatomical correlates to the bands seen in the outer retina by optical coherence tomography: literature review and model. *Retina*. 2011;31:1609–1619.
14. Staurenghi G, Sadda S, Chakravarthy U, Spaide RF. Proposed lexicon for anatomic landmarks in normal posterior segment spectral-domain optical coherence tomography: the IN•OCT consensus. *Ophthalmology*. 2014;121:1572–1578.
15. Shin HJ, Chung H, Kim HC. Association between foveal microstructure and visual outcome in age-related macular degeneration. *Retina*. 2011;31:1627–1636.
16. Sayanagi K, Sharma S, Kaiser PK. Photoreceptor status after antivascular endothelial growth factor therapy in exudative age-related macular degeneration. *Br J Ophthalmol*. 2009;93:622–626.
17. Landa G, Su E, Garcia PMT, Seiple WH, Rosen RB. Inner segment-outer segment junctional layer integrity and corresponding retinal sensitivity in dry and wet forms of age-related macular degeneration. *Retina*. 2011;31:364–370.
18. Hartmann KI, Bartsch D-UG, Cheng L, et al. Scanning laser ophthalmoscope imaging stabilized microperimetry in dry age-related macular degeneration. *Retina*. 2011;31:1323–1331.
19. Querques L, Querques G, Forte R, Souied EH. Microperimetric correlations of autofluorescence and optical coherence tomography imaging in dry age-related macular degeneration. *Am J Ophthalmol*. 2012;153:1110–1115.
20. Matsumoto H, Sato T, Kishi S. Outer nuclear layer thickness at the fovea determines visual outcomes in resolved central serous chorioretinopathy. *Am J Ophthalmol*. 2009;148:105–110.e1.
21. Murakami T, Tsujikawa A, Ohta M, et al. Photoreceptor status after resolved macular edema in branch retinal vein occlusion treated with tissue plasminogen activator. *Am J Ophthalmol*. 2007;143:171–173.
22. Chhablani J, Kim JS, Freeman WR, Kozak I, Wang HY, Cheng LY. Predictors of visual outcome in eyes with choroidal neovascularization secondary to age related macular degeneration treated with intravitreal bevacizumab monotherapy. *Indian J Ophthalmol*. 2013;6:62–66.
23. Oishi A, Shimozono M, Mandai M, Hata M, Nishida A, Kurimoto Y. Recovery of photoreceptor outer segments after anti-VEGF therapy for age-related macular degeneration. *Graefes Arch Clin Exp Ophthalmol*. 2013;251:435–440.
24. Subhi Y, Henningsen GO, Larsen CT, Sorensen MS, Sorensen TL. Foveal morphology affects self-perceived visual function and treatment response in neovascular age-related macular degeneration: a cohort study. *PLoS One*. 2014;9:e91227.
25. Hartmann KI, Gomez ML, Bartsch D-UG, Schuster AK, Freeman WR. Effect of change in drusen evolution on photoreceptor inner segment/outer segment junction. *Retina*. 2012;32:1492–1499.
26. Wu ZC, Ayton LN, Guymer RH, Luu CD. Second reflective band intensity in age-related macular degeneration. *Ophthalmology*. 2013;120:1307–1308.
27. Wu ZC, Ayton LN, Guymer RH, Luu CD. Relationship between the second reflective band on optical coherence tomography and multifocal electroretinography in age-related macular degeneration. *Invest Ophthalmol Vis Sci*. 2013;54:2800–2806.
28. Ferris FL III, Wilkinson CP, Bird A, et al. Clinical classification of age-related macular degeneration. *Ophthalmology*. 2013;120:844–851.
29. Fleckenstein M, Issa PC, Helb HM, et al. High-resolution spectral domain-OCT imaging in geographic atrophy associated with age-related macular degeneration. *Invest Ophthalmol Vis Sci*. 2008;49:4137–4144.
30. Wu Z, Luu CD, Ayton LN, et al. Optical coherence tomography–defined changes preceding the development of drusen-associated atrophy in age-related macular degeneration. *Ophthalmology*. 2014;121:2415–2422.
31. Querques G, Querques L, Martinelli D, et al. Pathologic insights from integrated imaging of reticular pseudodrusen in age-related macular degeneration. *Retina*. 2011;31:518–526.
32. Schmitz-Valckenberg S, Steinberg JS, Fleckenstein M, Visvalingam S, Brinkmann CK, Holz FG. Combined confocal scanning laser ophthalmoscopy and spectral-domain optical coherence tomography imaging of reticular drusen associated with age-related macular degeneration. *Ophthalmology*. 2010;117:1169–1176.
33. Ueda-Arakawa N, Ooto S, Tsujikawa A, Yamashiro K, Oishi A, Yoshimura N. Sensitivity and specificity of detecting reticular pseudodrusen in multimodal imaging in Japanese patients. *Retina*. 2013;33:490–497.
34. Vongkulsiri S, Suzuki M, Spaide RF. Colocalization error between the scanning laser ophthalmoscope infrared reflectance and optical coherence tomography images of the heidelberg spectralis. *Retina*. 2015;35:1211–1215.
35. Ross DH, Clark ME, Godara P, et al. RefMoB, a reflectivity feature model-based automated method for measuring four outer retinal hyperreflective bands in optical coherence tomography. *Invest Ophthalmol Vis Sci*. 2015;56:4166–4176.
36. Sundaram V, Wilde C, Aboshiha J, et al. Retinal structure and function in achromatopsia: implications for gene therapy. *Ophthalmology*. 2014;121:234–245.

Investigative Ophthalmology & Visual Science

37. Hu Z, Nittala MG, Sadda SR. Comparison of retinal layer intensity profiles from different OCT devices. *Ophthalmic Surg Lasers Imaging Retina*. 2013;44:S5–S10.
38. Lee SY, Stetson PF, Ruiz-Garcia H, Heussen FM, Sadda SR. Automated characterization of pigment epithelial detachment by optical coherence tomography. *Invest Ophthalmol Vis Sci*. 2012;53:164–170.
39. van der Schoot J, Vermeer KA, de Boer JF, Lemij HG. The effect of glaucoma on the optical attenuation coefficient of the retinal nerve fiber layer in spectral domain optical coherence tomography images. *Invest Ophthalmol Vis Sci*. 2012;53:2424–2430.
40. Lujan BJ, Roorda A, Knighton RW, Carroll J. Revealing Henle's fiber layer using spectral domain optical coherence tomography. *Invest Ophthalmol Vis Sci*. 2011;52:1486–1492.
41. Ho J, Witkin AJ, Liu J, et al. Documentation of intraretinal retinal pigment epithelium migration via high-speed ultra-high-resolution optical coherence tomography. *Ophthalmology*. 2011;118:687–693.
42. Cnaan A, Laird N, Slasor P. Tutorial in biostatistics: using the general linear mixed model to analyse unbalanced repeated measures and longitudinal data. *Stat Med*. 1997;16:2349–2380.
43. Yi K, Mujat M, Park BH, et al. Spectral domain optical coherence tomography for quantitative evaluation of drusen and associated structural changes in non-neovascular age-related macular degeneration. *Br J Ophthalmol*. 2009;176.
44. Zayit-Soudry S, Duncan JL, Syed R, Menghini M, Roorda AJ. Cone structure imaged with adaptive optics scanning laser ophthalmoscopy in eyes with nonneovascular age-related macular degeneration. *Invest Ophthalmol Vis Sci*. 2013;54:7498–7509.
45. Zweifel SA, Spaide RF, Curcio CA, Malek G, Imamura Y. Reticular pseudodrusen are subretinal drusenoid deposits. *Ophthalmology*. 2010;117:303–312.e1.
46. Querques G, Canoui-Poitrine F, Coscas F, et al. Analysis of progression of reticular pseudodrusen by spectral domain-optical coherence tomography. *Invest Ophthalmol Vis Sci*. 2012;53:1264–1270.
47. Christenbury JG, Folgar FA, O'Connell RV, Chiu SJ, Farsiu S, Toth CA. Progression of intermediate age-related macular degeneration with proliferation and inner retinal migration of hyperreflective foci. *Ophthalmology*. 2013;120:1038–1045.
48. Folgar FA, Chow JH, Farsiu S, et al. Spatial correlation between hyperpigmentary changes on color fundus photography and hyperreflective foci on SDOCT in intermediate AMD. *Invest Ophthalmol Vis Sci*. 2012;53:4626–4633.
49. Kenney MC, Hertzog D, Chak G, et al. Mitochondrial DNA haplogroups confer differences in risk for age-related macular degeneration: a case control study. *BMC Med Genet*. 2013;14:1–9.
50. Jones MM, Manwaring N, Wang JJ, Rochtchina E, Mitchell P, Sue CM. Mitochondrial DNA haplogroups and age-related maculopathy. *Arch Ophthalmol*. 2007;125:1235–1240.
51. Hoang QV, Linsenmeier RA, Chung CK, Curcio CA. Photoreceptor inner segments in monkey and human retina: mitochondrial density, optics, and regional variation. *Vis Neurosci*. 2002;19:395–407.
52. Meadway A, Girkin CA, Zhang Y. A dual-modal retinal imaging system with adaptive optics. *Opt Express*. 2013;21:29792–29807.
53. Jonnal RS, Kocaoglu OP, Zawadzki RJ, Lee S-H, Werner JS, Miller DT. The cellular origins of the outer retinal bands in optical coherence tomography images. *Invest Ophthalmol Vis Sci*. 2014;55:7904–7918.
54. Putnam NM, Hammer DX, Zhang Y, Merino D, Roorda A. Modeling the foveal cone mosaic imaged with adaptive optics scanning laser ophthalmoscopy. *Opt Express*. 2010;18:24902–24916.
55. Litts KM, Messinger JD, Freund KB, Zhang Y, Curcio CA. Inner segment remodeling and mitochondrial translocation in cone photoreceptors in age-related macular degeneration with outer retinal tubulation. *Invest Ophthalmol Vis Sci*. 2015;56:2243–2253.
56. Schaal KB, Freund KB, Litts KM, Zhang Y, Messinger JD, Curcio CA. Outer retinal tubulation in advanced age-related macular degeneration: optical coherence tomographic findings correspond to histology. *Retina*. 2015;35:1339–1350.
57. Litts KM, Messinger JD, Dellatorre K, Yannuzzi LA, Freund K, Curcio CA. Clinicopathologic correlation of outer retinal tubulation in age-related macular degeneration. *JAMA Ophthalmol*. 2015;133:609–612.
58. Birch DG, Wen YQ, Locke K, Hood DC. Rod sensitivity, cone sensitivity, and photoreceptor layer thickness in retinal degenerative diseases. *Invest Ophthalmol Vis Sci*. 2011;52:7141–7147.

Investigative Ophthalmology & Visual Science